Predictions of characteristics of prompt-fission γ-ray spectra from the $n + {}^{238}$U reaction up to $E_n = 20$ MeV

A. Oberstedt,[1] R. Billnert,[2,*] and S. Oberstedt[2,†]

[1]*Extreme Light Infrastructure–Nuclear Physics (ELI-NP)/Horia Hulubei National Institute for Physics and Nuclear Engineering (IFIN-HH), R-077125 Bucharest-Magurele, Romania*

[2]*European Commission, DG Joint Research Centre, Directorate G–Nuclear Safety and Security, Unit G.2 Standards for Nuclear Safety, Security and Safeguards, B-2440 Geel, Belgium*

(Received 23 September 2016; revised manuscript received 4 September 2017; published 19 September 2017)

Systematics from 2001, describing prompt-fission γ-ray spectra (PFGS) characteristics as a function of mass and atomic number of the fissioning system, was revisited and parameters were revised, based on recent experimental results. Although originally expressed for spontaneous and thermal-neutron induced fission, validity for fast neutrons was assumed and applied to predict PFGS characteristics for the reaction $n + {}^{238}$U up to incident neutron energies of $E_n = 20$ MeV. The results from this work are in good agreement with corresponding results from both model calculations and experiments.

DOI: 10.1103/PhysRevC.96.034612

I. INTRODUCTION

A bit more than a decade ago an evaluation of prompt-fission γ-ray spectra (PFGS) was presented, trying to describe the average total γ-ray energy released in fission as well as the average energy per emitted γ ray as functions of mass and atomic number, A and Z, of the fissioning system [1]. From both characteristic properties, even the average γ-ray multiplicity was deduced. Based on thitherto available experimental data for ^{233}U$(n_{\rm th}, f)$ [2], ^{235}U$(n_{\rm th}, f)$ [3–5], ^{239}Pu$(n_{\rm th}, f)$ [2,4], and ^{252}Cf(sf) [4,6–9] A and Z dependencies were found "by trial and error," without any physical significance [1]. Nevertheless, the description given there offers the possibility to estimate average properties of PFGS for fissioning systems, which are difficult or virtually impossible to access experimentally.

However, in recent years the measurement of PFGS has undergone a renaissance, motivated by requests for new precise values especially for γ-ray multiplicities and average photon energy release per fission in the thermal-neutron induced fission of ^{235}U and ^{239}Pu [10]. Two experimental groups, a collaboration involving JRC Geel (formerly known as IRMM)/Chalmers/Budapest and others as well as another between Los Alamos and Livermore, reported on results from ^{252}Cf(sf) [11,12] and ^{235}U$(n_{\rm th}, f)$ [13,14], ^{239,241}Pu$(n_{\rm th}, f)$ [15,16], and ^{240,242}Pu(sf) [17] as well as ^{252}Cf(sf) [18–20], ^{235}U(n, f) [19,20], and ^{239,241}Pu(n, f) [19–21], respectively. A comparison of all results for the PFGS properties from ^{252}Cf(sf) [12], ^{235}U$(n_{\rm th}, f)$ [13], and ^{241}Pu$(n_{\rm th}, f)$ [16] exhibits deviations, which motivated an investigation of the influence of the recent measurements on the evaluation in Ref. [1]. This will be discussed in the following section. This evaluation was obviously performed for thermal-neutron induced and spontaneous fission, on which the systematics is based. Hence, it may be assumed to be valid for excitation energies of the fissioning system ranging from zero to the neutron separation energy. Below we extend the revised systematics to fast neutron induced fission and apply it to the system $n + {}^{238}$U, which is highly relevant for fast reactor applications and involves one of the six important isotopes in the focus of the Collaborative International Evaluated Library Organization (CIELO) Pilot Project of the OECD/NEA [22]. The predicted PFGS characteristics for this system up to 20-MeV incident neutron energy are then compared to results from theoretical calculations and recent measurements.

II. REVISED SYSTEMATICS FOR PFGS CHARACTERISTICS

In Ref. [1], an attempt was made to find a consistent parametrization of PFGS characteristics for different fissioning systems, expressed as a function of their mass and atomic numbers as well as their prompt-fission neutron multiplicity. Because this is related to the de-excitation mechanism of the fission fragments, we give a brief summary below. Then we motivate why we believe that the original systematics has to be revised because of the appearance of new experimental PFGS data, followed by a presentation of the resulting updated systematics.

A. De-excitation of fission fragments

The de-excitation of fission fragments in the very stage, i.e., within less than 10 ns after scission, takes place by the emission of neutrons and γ rays, which both contribute to the so-called prompt heat released in the fission process. Comprehensive experimental studies of the de-excitation mechanism of the fission fragments from ^{252}Cf(sf) have already been performed in 1972 [23]. In a multiparameter experiment the kinetic energies of the fragments, the number of prompt neutrons ($\overline{\nu}_n$) and the total γ-ray energy per fission ($E_{\gamma,\rm tot}$) were measured and correlations were observed. For instance, for individual fission fragment masses the emitted γ-ray energy decreases linearly with increasing kinetic energy of the fragment, which

*Present address: Studsvik Nuclear Environmental AB, 611 82 Nyköping, Sweden.

†stephan.oberstedt@ec.europa.eu

is in agreement with the observed dependence of the total γ-ray energy averaged over all fragments.[1] The observed dependence between emitted γ-ray and kinetic energy may be understood with the fact that the kinetic energy of a fragment is reduced in favor of a higher excitation energy. At the same time, the higher excitation energy the more prompt-fission neutrons are emitted. Hence, $E_{\gamma,\mathrm{tot}}$ should increase with $\overline{\nu}_n$, according to a dependence that was observed to be linear one [23]. Another linear dependence that was observed in the same measurement, describes the relation between the average prompt-fission γ-ray multiplicity ($\overline{M}_\gamma$) and $\overline{\nu}_n$. This, in turn, implies that the average energy of an emitted γ ray (ϵ_γ) should be independent of $\overline{\nu}_n$.

B. PFGS characteristics for different systems

If all the above mentioned is true for individual fission fragments (for which there is experimental evidence), it must also be possible to be applied to the fissioning system, which corresponds to averaging over its entire fission fragment distribution. To extend the observations made for the spontaneous fission of ^{252}Cf to other fissioning systems, an additional dependence from both mass and atomic number, A and Z, respectively, was introduced [1]. The suggested description for $E_{\gamma,\mathrm{tot}}(\overline{\nu}_n,Z,A)$ in MeV, based on the study published in Ref. [23], becomes then of the form,

$$E_{\gamma,\mathrm{tot}}(\overline{\nu}_n,Z,A) = \varphi(Z,A) \times \overline{\nu}_n + 4.0, \quad (1)$$

with

$$\varphi(Z,A) = a_0 + a_1 \times Z^2 A^{1/2}. \quad (2)$$

The parameters a_0 and a_1 were determined by a least-squares fit to experimental data, while the values for $\overline{\nu}_n$ had been taken from experiments [1]. The average energy per emitted γ ray, ϵ_γ, was assumed to be independent from $\overline{\nu}_n$ and depending on A and Z according to

$$\epsilon_\gamma(Z,A) = b_0 + b_1 \times Z^{1/3} A^{-1}. \quad (3)$$

Here too, the parameters b_0 and b_1 were determined by a fit to experimental results. A relation for the average prompt-fission γ-ray multiplicity $\overline{M}_\gamma$ may then be inferred by dividing Eq. (1) with Eq. (3) and using Eq. (2). Although different functions may be used to approximate $\overline{M}_\gamma(\overline{\nu}_n,Z,A)$, we have chosen

$$\overline{M}_\gamma(\overline{\nu}_n,Z,A) = [c_0 + c_1 \times Z^{5/3} A^{-1/2}] \times \overline{\nu}_n, \quad (4)$$

to present experimental values graphically. Figure 1 gives an overview of all experimental results for (a) $E_{\gamma,\mathrm{tot}}(\overline{\nu}_n,Z,A)$, (b) $\epsilon_\gamma(Z,A)$, and (c) $\overline{M}_\gamma(\overline{\nu}_n,Z,A)$ in accordance with the above given equations. The dashed (black) lines correspond to the evaluation in Ref. [1], based on experimental results that were reported until 1973 (the references are given in Ref. [1]), denoted by full drawn (black) circles. The (blue) open squares indicate the results obtained by the Los Alamos/Livermore

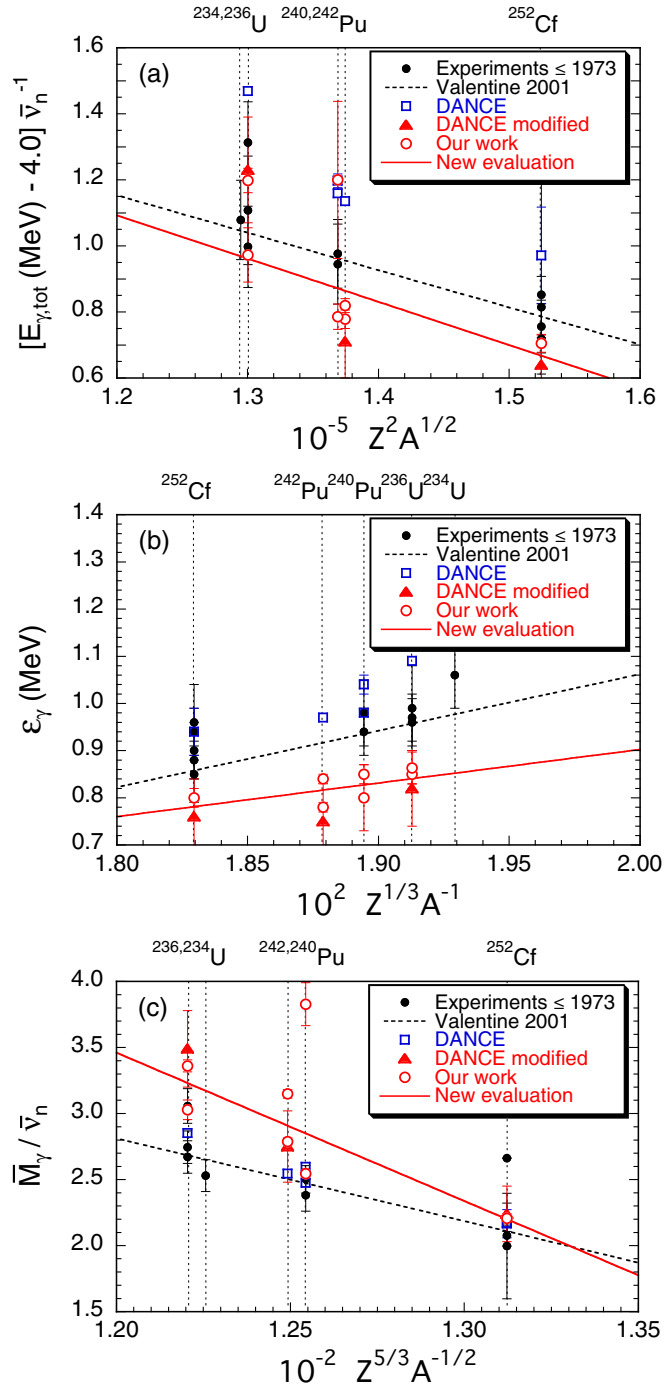

FIG. 1. Overview of experimental results for the average total γ-ray energy released in fission (upper part), the average energy per photon (middle part), and prompt-fission γ-ray multiplicity (lower part) as function of A and Z for different fissioning systems. Full (black) circles denote historical results [2–9], open (blue) squares indicate results obtained with DANCE [18–21], and open (red) circles represent results from our previous work [11–17]. The (red) triangles correspond to a modification of the results in Refs. [18–21]; see text for details. Also shown are results from evaluations by Valentine [1] (dashed black line) and from this work (full drawn red line), based on the historical data and our previous results, respectively. For the sake of clarity, the corresponding fissioning systems are given, too.

[1]By the way, for the average total γ-ray energy per fission a value of 6.82 MeV is given [23], which is in pretty good agreement with a recent measurement, resulting in $E_{\gamma,\mathrm{tot}} = (6.65 \pm 0.10)$ MeV [12].

collaboration [18–21] by using the DANCE detector system [24], while the (red) triangles correspond to modifications of these data according to a procedure that was described in Ref. [12]. There it was shown for ^{252}Cf(sf) that the PFGS from Ref. [18] is missing 30% of predominantly low energy photons, i.e., γ rays with energies below 500 keV, which is leading to mean energy values which are too high compared to all others observed for this fissioning system. Correction factors were determined and applied, resulting in values in good agreement with not only all other experiments but also with measured distributions actually published in Ref. [18]. In the same way the results for ^{235}U$(n_{\rm th},f)$ and ^{241}Pu$(n_{\rm th},f)$ [19] were corrected based on the results in Refs. [13,16], respectively. Our results, also recently published [11–17], are shown as (red) open circles. The values for $\overline{\nu}_n$ were taken as given in Ref. [1]. Because of obvious discrepancies between the historical and the recently obtained experimental data, a new evaluation seems to be reasonable on the basis of these new results. However, even those exhibit considerable differences as mentioned above, depending on by which experimental group they were obtained. Hence, only values from our previous work and the modified results obtained with DANCE were included in a new evaluation. By this selection we make sure that all considered data was obtained under the same experimental conditions. As far as our previous results are concerned, depicted as open (red) circles, all spectra had in common a low energy threshold of 100 keV and a high energy limit of at least 6 MeV. Including even higher γ-ray energies has a negligible effect on PFGS characteristics, as shown in Ref. [13]. The chosen timing window for prompt γ rays had in all our measurements the same width relative to the individually observed coincidence timing resolution (FWHM). Hence, all our results are consistent with each other. The same is assumed to be true for all data taken with DANCE, because in each of those measurements the same, fixed instrumentation was used. This assumption is corroborated by the fact that the corrections originally found for and applied to a ^{252}Cf(sf) spectrum [12] give the same good agreement with our results also for other fissioning systems, as indicated by the red triangles.

The results of this new evaluation are depicted by full drawn (red) lines in Fig. 1. They were obtained by least-squares fits, weighted with the uncertainties, to the experimental results specified above, leading to the following description of the average total γ-ray energy released in fission in MeV,

$$E_{\gamma,\rm tot}(\overline{\nu}_n,Z,A) = [(2.66\pm0.19) - (1.31\pm0.13)\times10^{-5} \times Z^2A^{1/2}]\times\overline{\nu}_n + 4.0, \quad (5)$$

and the average energy per photon in MeV,

$$\epsilon_\gamma(Z,A) = (-0.52\pm0.56) + (0.71\pm0.30) \times 10^2 \times Z^{1/3}A^{-1}, \quad (6)$$

while the average prompt-fission γ-ray multiplicity may be approximated by

$$\overline{M}_\gamma(\overline{\nu}_n,Z,A) = [(16.9\pm0.4) - (11.2\pm0.3) \times10^{-2}\times Z^{5/3}A^{-1/2}]\times\overline{\nu}_n. \quad (7)$$

Although the fit parameters are afflicted with considerable uncertainties, basically because of the fact that only few experimental data were considered for the new evaluation, the differences compared to the one in Ref. [1] are quite obvious. We have to point out that the fit results presented here deviate also from the ones previously reported by us (see, e.g., Refs. [25,26]), which is because of the fact that in this work more data were available to be taken into consideration (modified DANCE data, ^{240,242}Pu(sf) [17], ^{239}Pu$(n_{\rm th},$f) [15] as well as ^{235}U$(n_{\rm th},f)$ [14]). A final judgment has to be the subject of further experimental studies, which then have to be included in the systematics presented here. For the time being, we emanate from the equations presented above to predict PFGS properties for the system $n+^{238}$U.

III. THE SYSTEM $n+^{238}$U AT $E_n \leqslant 20$ MeV

From the systematics of PFGS characteristics presented in the previous section it should be possible to interpolate to any fissioning system. The only apparent energy dependence is an implicit one, hidden in the prompt-fission neutron multiplicity. If this one is known, there is no obvious reason why the validity of this systematics should be restricted to spontaneous or thermal-neutron induced fission. Hence, in the following we apply the systematics to fission induced by fast neutrons on ^{238}U in the energy range from 0 to 20 MeV. The energy dependence of the prompt-fission neutron multiplicity was assumed to be a linear one [27] and recent data may be found in the evaluated library ENDF/B-VII.1 [28]. However, in the considered energy range channels for multichance fission may be open, leading to the emission of pre-fission neutrons. Because these neutrons are not emitted from fission fragments but the compound system, they do not contribute to the de-excitation of the fragments in competition with prompt γ-ray emission. However, as shown in Ref. [29], they are included in the numbers given in the evaluated files. Hence, pre-fission neutrons have to be assessed and subtracted to obtain proper values to be used in the systematics above. This will be done below.

A. Correction for pre-fission neutrons

As already shown in Ref. [23] for ^{252}Cf(sf), the total γ-ray energy released in fission (and the γ-ray multiplicity) is increasing linearly with the average number of neutrons emitted per fission, i.e., $\overline{\nu}_n$. The same behavior may be inferred for ^{235}U(n,f) and ^{238}U(n,f) from Ref. [27], where a linear increase of both total γ-ray energy and average prompt neutron multiplicity with incident neutron energy is reported. In Ref. [29], however, it was shown for the neutron induced fission of ^{235}U that this is only true as long as the (n,f) channel is considered. Hence, for neutron energies above the neutron separation energy of the compound system, the channels for second, third, etc., fission, i.e., $(n,$nf$)$, $(n,2$nf$)$ and so on, may be open and the neutrons emitted prior to fission of the corresponding residual compound systems have to be subtracted from the total number of prompt-fission neutrons.

For the system $n+^{238}$U, the threshold for the $(n,$nf$)$ channel is at $E_n = S_n(^{239}\text{U}) = 4.807$ MeV, while the

$(n,2nf)$ channel becomes possible above $E_n = S_{2n}(^{239}\mathrm{U}) = S_n(^{239}\mathrm{U}) + S_n(^{238}\mathrm{U}) = (4.807 + 6.152)\,\mathrm{MeV} = 10.959\,\mathrm{MeV}$ and the $(n,3nf)$ channel above $E_n = S_{3n}(^{239}\mathrm{U}) = S_n(^{239}\mathrm{U}) + S_n(^{238}\mathrm{U}) + S_n(^{237}\mathrm{U}) = (4.807 + 6.152 + 5.126)\,\mathrm{MeV} = 16.085\,\mathrm{MeV}$. The neutron separation energies S_n were calculated from a mass table, like the one in Ref. [30]. Hence, for a given incident neutron energy, several fissioning systems (^{239}U*, ^{238}U*, ^{237}U*, ...) are possible, depending on the threshold conditions mentioned before.

For a neutron with given E_n captured by a ^{238}U nucleus, one obtains an excitation energy E_x of the compound system $A_{\mathrm{CN}} = 239$, which may be expressed as

$$\begin{aligned} E_x(A_{\mathrm{CN}}) &= S_n(A_{\mathrm{CN}}) + E_n \\ &= aT^2, \end{aligned} \tag{8}$$

where T denotes the nuclear temperature of A_{CN} and the level density parameter $a = A_{\mathrm{CN}}/7.524\,\mathrm{MeV}^{-1}$ was inferred from Ref. [29]. When a neutron is emitted from A_{CN}, its average kinetic energy is given by $\langle E_n \rangle = 3/2\,\mathrm{T}$, which may be calculated from the excitation energy $E_x(A_{\mathrm{CN}})$. Here, a Maxwellian evaporation spectrum is assumed. This leaves the residual system A_{CN}-1 in an excited state, whose average excitation energy corresponds to a situation, where a nucleus with A_{CN}-2 has absorbed a neutron of incident energy E'_n. Hence,

$$\begin{aligned} E_x(A_{\mathrm{CN}} - 1) &= S_n(A_{\mathrm{CN}} - 1) + E'_n \\ &= E_x(A_{\mathrm{CN}}) - S_n(A_{\mathrm{CN}}) - \langle E_n \rangle \\ &= a'T'^2. \end{aligned} \tag{9}$$

Again, a neutron may be emitted, this time with an average energy $\langle E'_n \rangle = 3/2\,T'$, where A_{CN} is replaced by A_{CN}-1 in a'. Consequently, after further neutron emission remains a compound system A_{CN}-2 with

$$\begin{aligned} E_x(A_{\mathrm{CN}} - 2) &= S_n(A_{\mathrm{CN}} - 2) + E''_n \\ &= E_x(A_{\mathrm{CN}} - 1) - S_n(A_{\mathrm{CN}} - 1) - \langle E'_n \rangle \\ &= a''T''^2, \end{aligned} \tag{10}$$

corresponding to a nucleus with A_{CN}-3 after absorbing a neutron of energy E''_n. After another neutron emission with $\langle E''_n \rangle$, this procedure may be extended to higher fission channels. The total average prompt-fission neutron multiplicity $\overline{\nu}_n^{239}(E_n)$ for the system $n + ^{238}$U at a given energy E_n, as given in evaluated libraries, may then be decomposed into contributions from the different fission channels,

$$\overline{\nu}_n^{239}(E_n) = \overline{\nu}_{(n,f)}^{239}(E_n) + \overline{\nu}_{(n,nf)}^{239}(E_n) + \overline{\nu}_{(n,2nf)}^{239}(E_n) + \ldots, \tag{11}$$

where the superscripts from now on indicate the mass number of the actual compound nucleus. Considering the fact that $\overline{\nu}_n$ contains both pre-fission neutrons $\overline{\nu}_{\mathrm{pre}}$ and neutrons actually emitted from fission fragments $\overline{\nu}_{ff}$ according to

$$\overline{\nu}_n = \overline{\nu}_{\mathrm{pre}} + \overline{\nu}_{ff}, \tag{12}$$

the individual contributions in Eq. (11) for $n + ^{238}$U may be related to the multiplicities for the first-chance fission of the different fissioning systems at the corresponding energies and weighted with the probabilities for each fission channel,

$$\begin{aligned} \overline{\nu}_{(n,f)}^{239}(E_n) &= \left(\overline{\nu}_{ff}^{239}(E_n) + 0\right) \times \frac{\sigma_{(n,f)}^{239}(E_n)}{\sigma_{\mathrm{fission}}^{239}(E_n)}, \\ \overline{\nu}_{(n,nf)}^{239}(E_n) &= \left(\overline{\nu}_{ff}^{238}(E'_n) + 1\right) \times \frac{\sigma_{(n,nf)}^{239}(E_n)}{\sigma_{\mathrm{fission}}^{239}(E_n)}, \\ \overline{\nu}_{(n,2nf)}^{239}(E_n) &= \left(\overline{\nu}_{ff}^{237}(E''_n) + 2\right) \times \frac{\sigma_{(n,2nf)}^{239}(E_n)}{\sigma_{\mathrm{fission}}^{239}(E_n)}. \end{aligned} \tag{13}$$

In the range considered in this work, only first-, second-, and third-chance fission play a major role, because the onset of fourth-chance fission is at about $E_n = 18\,\mathrm{MeV}$. The prompt-fission neutron multiplicities for $n + ^{238}$U, $n + ^{237}$U, and $n + ^{236}$U (denoted by $\overline{\nu}_n^{239}$, $\overline{\nu}_n^{238}$, and $\overline{\nu}_n^{237}$, respectively) were taken from ENDF/B-VII.1 [28,31,32] as displayed in Fig. 2. The figures 0, 1, and 2 in Eq. (13) denote the number of emitted neutrons prior to fission (i.e., pre-fission neutrons) in case of first-, second-, and third-chance fission, respectively. The corresponding probabilities are given by the cross section ratios in Eq. (13). The values for $\sigma_{\mathrm{fission}}^{239}(E_n)$ were also taken from ENDF/B-VII.1 [33], while the contributions from the individual fission channels were estimated recursively. At the onset of second-chance fission, a $1/\sqrt{E}$ dependence, motivated by the general energy dependence of cross sections for neutron induced reactions as given in textbooks like Ref. [30], was adjusted to the total fission cross section to describe the component for first-chance fission. This component was then subtracted from the total fission cross section and the result was treated in the same way to find the component for second-chance fission. The remaining component was then assumed to correspond to third-chance fission. The total fission cross section $\sigma_{\mathrm{fission}}^{239}(E_n)$ together with its components is depicted in Fig. 3. We have chosen this procedure for two reasons: (1) cross section data sets for the fission of $n + ^{238}$U in the different evaluated libraries show quite deviating values, in

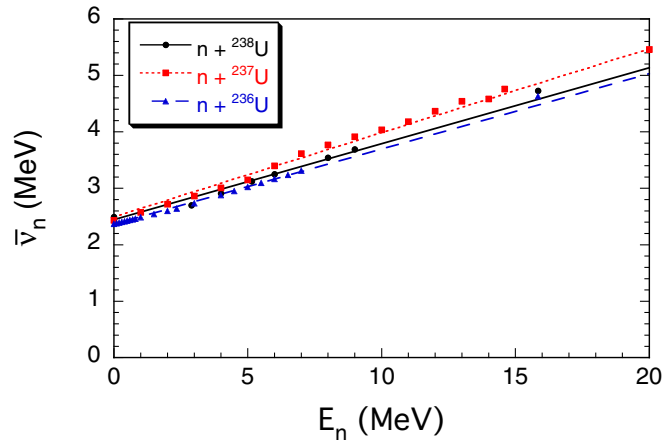

FIG. 2. Prompt-fission neutron multiplicities for $n + ^{238}$U (black circles), $n + ^{237}$U (red squares), and $n + ^{236}$U (blue triangles) as function of incident neutron energy as found in ENDF/B-VII.1. The different lines represent the result of linear fits to interpolate values for any neutron energy.

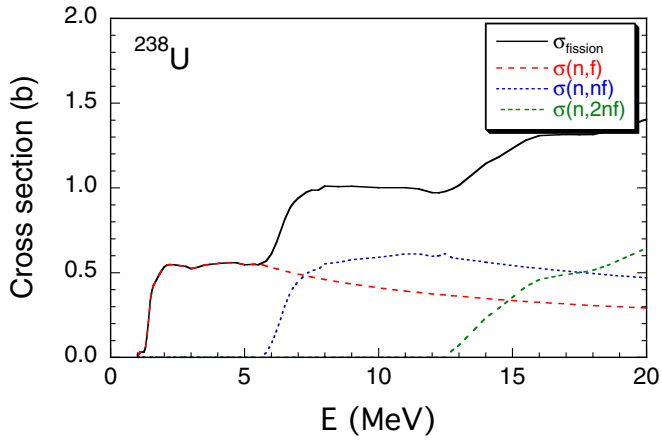

FIG. 3. Energy dependent cross sections for fast neutron induced fission of ^{238}U. The total fission cross section (full drawn black line) was taken from ENDF/B-VII.1, while the components for first-, second-, and third-chance fission were extracted according to the procedure described in the text.

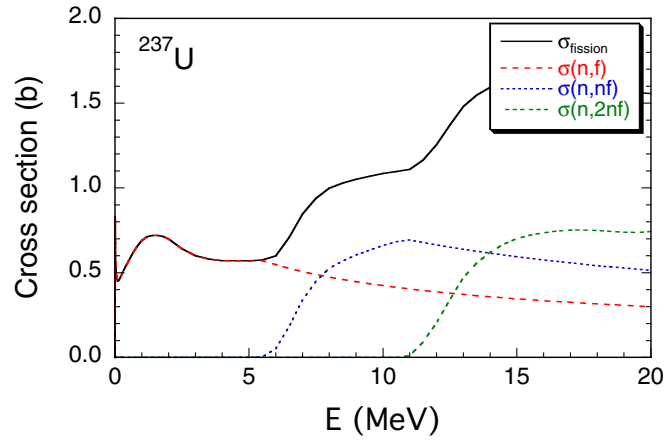

FIG. 4. Energy dependent cross sections for fast neutron induced fission of ^{237}U. The total fission cross section was taken from ENDF/B-VII.1; the different components are results from the procedure described in the text. The presentation is the same as in Fig. 3.

particular for the second-chance fission in ENDF/B-VII.1 and JENDL-4.0 [34,35]; (2) we were aiming at finding a technique that may also be applied to nuclei, for which no evaluated cross-section data are available. This technique was tested for the multichance fission of $n + {}^{233}$Pa [36], where the different fission channels were calculated, with excellent agreement.

For the total prompt-fission neutron multiplicity $\overline{\nu}_n^{238}(E_n')$ for the system $n + {}^{237}$U, both first- and second-chance fission have to be taken into account,

$$\overline{\nu}_n^{238}(E_n') = \overline{\nu}_{(n,f)}^{238}(E_n') + \overline{\nu}_{(n,nf)}^{238}(E_n'), \tag{14}$$

requiring a decomposition similar to Eq. (13),

$$\overline{\nu}_{(n,f)}^{238}(E_n') = \left(\overline{\nu}_{ff}^{238}(E_n') + 0\right) \times \frac{\sigma_{(n,f)}^{238}(E_n')}{\sigma_{\text{fission}}^{238}(E_n')},$$
$$\overline{\nu}_{(n,nf)}^{238}(E_n') = \left(\overline{\nu}_{ff}^{237}(E_n'') + 1\right) \times \frac{\sigma_{(n,nf)}^{238}(E_n')}{\sigma_{\text{fission}}^{238}(E_n')}. \tag{15}$$

Figure 4 shows the total fission cross section $\sigma_{\text{fission}}^{238}(E_n)$ for $n + {}^{237}$U taken from ENDF/B-VII.1 [33], together with the components for first-, second-, and third-chance fission, obtained according to the procedure described above. For the fast neutron induced fission of ^{236}U, such a decomposition is not really necessary, because the maximum energy for $\langle E_n'' \rangle$ considered here is just around the threshold for second-chance fission. Hence, values for $\overline{\nu}_n^{237}(E_n'')$ may be taken directly from ENDF/B-VII.1 [32], as depicted in Fig. 2, and hence the real number of prompt neutrons per fission emitted from the fragments is given by

$$\overline{\nu}_{ff}^{237}(E_n'') = \overline{\nu}_n^{237}(E_n''). \tag{16}$$

Using this result and combining Eqs. (14) and (15), the equivalent value $\overline{\nu}_{ff}^{238}(E_n')$ may be determined by

$$\overline{\nu}_{ff}^{238}(E_n') = \left[\overline{\nu}_n^{238}(E_n') \times \sigma_{\text{fission}}^{238}(E_n') - \left(\overline{\nu}_n^{237}(E_n'') + 1\right) \times \sigma_{(n,nf)}^{238}(E_n')\right] \Big/ \sigma_{(n,f)}^{238}(E_n'), \tag{17}$$

where the cross sections correspond to the ones shown in Fig. 4. Combining Eqs. (11) and (13) and using the results for $\overline{\nu}_{ff}^{237}(E_n'')$ and $\overline{\nu}_{ff}^{238}(E_n')$ according to Eqs. (16) and (17), $\overline{\nu}_{ff}^{239}(E_n)$ is determined by

$$\overline{\nu}_{ff}^{239}(E_n) = \left[\overline{\nu}_n^{239}(E_n) \times \sigma_{\text{fission}}^{239}(E_n) - \left(\overline{\nu}_n^{238}(E_n') + 1\right) \times \sigma_{(n,nf)}^{239}(E_n) - \left(\overline{\nu}_n^{237}(E_n'') + 2\right) \times \sigma_{(n,2nf)}^{239}(E_n)\right] \Big/ \sigma_{(n,f)}^{239}(E_n). \tag{18}$$

Summarizing the results from Eqs. (16)–(18), the total average number of prompt neutrons $\overline{\nu}_{ff}(E_n)$ emitted by fragments per multiple chance fission of $n + {}^{238}$U may be calculated according to

$$\overline{\nu}_{ff}(E_n) = \left[\overline{\nu}_{ff}^{239}(E_n) \times \sigma_{(n,f)}^{239}(E_n) + \overline{\nu}_{ff}^{238}(E_n') \times \sigma_{(n,nf)}^{239}(E_n) + \overline{\nu}_{ff}^{237}(E_n'') \times \sigma_{(n,2nf)}^{239}(E_n)\right] \Big/ \sigma_{\text{fission}}^{239}(E_n). \tag{19}$$

We would like to remind one of the relations between E_n, E_n', and E_n'' given by Eqs. (8), (9), and (10). The result for $E_n = 0$–20 MeV is shown in Fig. 5 as the (red) dotted line, together with the average total prompt-fission multiplicity from ENDF/B-VII.1 [28] (solid line). The pre-fission neutron multiplicity $\overline{\nu}_{\text{pre}}$, given by the difference of both, is shown as well as the dashed (blue) line. Again, we would like to emphasize that only the prompt neutrons emitted from fission fragments are competing with prompt-fission γ-ray emission in the de-excitation of fission fragments. Below we apply our findings to the systematics presented in Sec. II to predict PFGS properties.

B. Energy dependence of PFGS characteristics

From the revised systematics presented in Sec. II, PFGS properties may be inferred for the fissioning system $n + {}^{238}$U. Equation (5) with $Z = 92$ and $A = 239$ in conjunction with the neutron multiplicity according to Eq. (18) allows calculating the average total γ-ray energy released in fission as a function of incident neutron energy. The result is denoted as prediction and depicted in Fig. 6 together with a linear

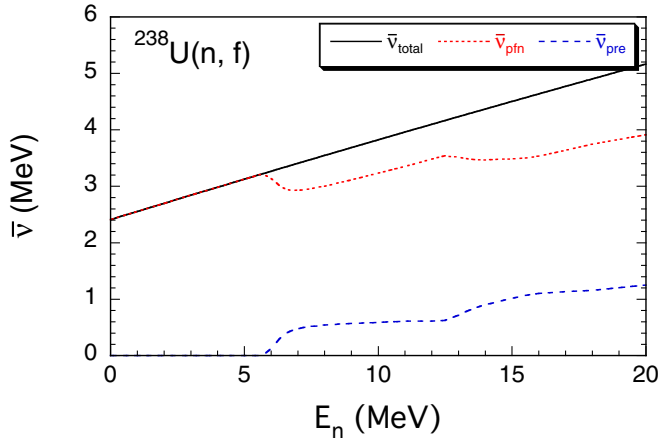

FIG. 5. Average prompt-fission neutron multiplicity for $n + {}^{238}\mathrm{U}$ as given in ENDF/B-VII.1 (full drawn black line) together with the components from neutrons actually emitted by fission fragments (dotted red line) and evaporated prior to fission (dashed blue line).

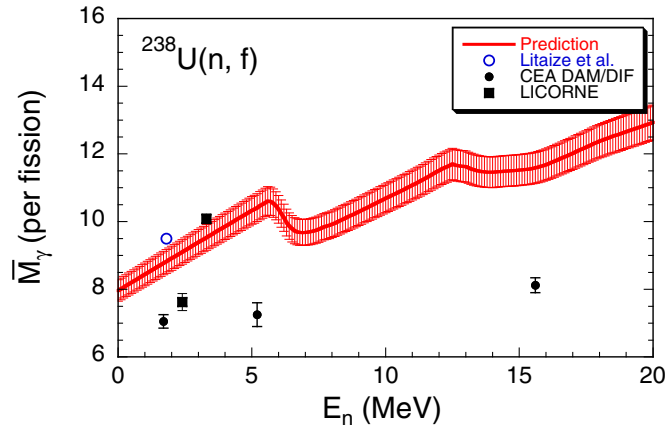

FIG. 7. Predicted average prompt-fission γ-ray multiplicity for $n + {}^{238}\mathrm{U}$ from this work as function of incident neutron energy (full drawn red line). For comparison, a theoretical result from Refs. [39,40] and experimental results from Refs. [45,48] are shown as open (blue) and full (black) circles and squares, respectively.

fit to an empirical approach from Ref. [27]. The (blue) open circle denotes a calculated result obtained with the Monte Carlo Hauser-Feshbach model FIFRELIN [37,38] for $E_n = 1.8$ MeV, previously reported in Refs. [39,40]. The (green) squares and triangles represent results from calculations [41] in the framework of the Point-by-Point model (for details see, e.g., Ref. [42] and references therein). The (green) dashed line indicates results from the most recent calculations based on the same model [41], however, with model parameters used in Ref. [43]. Experimental results are scarce for the fissioning system considered in this work, but two measurements were reported at $E_n = 1.7$ and 15.6 MeV [44]. In the meantime two more experiments were performed at $E_n = 1.7$ and 5.2 MeV and a publication is under way [45]. These results are depicted as full (black) circles. Some years ago, the directional neutron source LICORNE has become operational [46] and first experiments have successfully been performed [47]. Preliminary results for $E_n = 2.4$ and 3.3 MeV [48] are also shown in Fig. 6 as full (black) squares.

Figure 7 shows our prediction for the average prompt-fission γ-ray multiplicity as a function of incident neutron energy, derived by combining Eq. (7) with Eq. (18). One calculated value was available [39,40], again depicted as (blue) open circle, and the experimental results from Refs. [45,48] (full black circles and squares) are shown as well for comparison. Figure 8 finally contains our predictions for the average γ-ray energy per fission as a function of incident neutron energy, obtained by dividing Eq. (5) with Eq. (7).

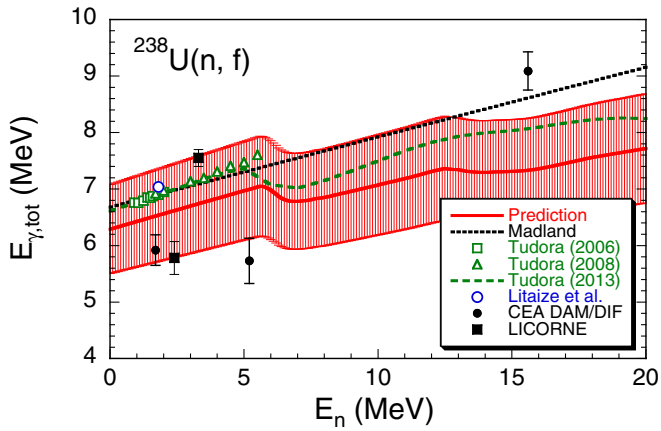

FIG. 6. Predicted average total γ-ray energy released in the fission of $n + {}^{238}\mathrm{U}$ (full drawn red line) from this work as function of incident neutron energy. First experimental results from Refs. [45,48] (full black circles and squares, respectively), a linear approximation from Ref. [27] (dotted black line) as well as results from calculations by Ref. [39,40] (open blue circle) and Ref. [41] (green open squares and triangles and dashed line) are shown, too.

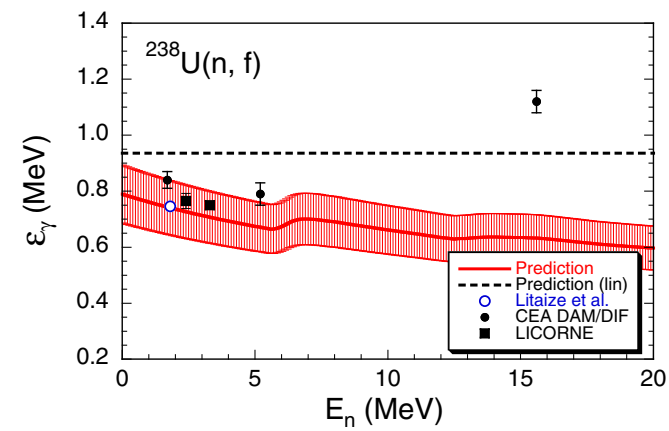

FIG. 8. Predicted average γ-ray energy per fission for $n + {}^{238}\mathrm{U}$ from this work as a function of incident neutron energy (full drawn red line), obtained by dividing the values in Fig. 6 with the ones in Fig. 7. A constant approach is depicted as a dashed (black) line, while a theoretical result from Refs. [39,40] and preliminary experimental results from Refs. [45,48] are shown as open (blue) and full (black) circles and squares, respectively.

Equation (6) predicts a constant value, which is indicated by the (black) dashed line. Again the corresponding experimental and theoretical results from the previous figure are shown in addition. A discussion of our results and concluding remarks follow below.

IV. DISCUSSION AND CONCLUSIONS

In the previous section we have presented the results from our predictions of PFGS characteristics for the system $n + {}^{238}\mathrm{U}$ in the incident neutron energy range $E_n = 0$–20 MeV. The average total γ-ray energy released in fission $E_{\gamma,\mathrm{tot}}(E_n)$ was compared to values obtained from an interpolation of empirical data [27] and theoretical calculations [40,41]. The latter ones (i.e., those indicated by symbols) cover only the region up to the threshold for second-chance fission, but there the agreement with our predictions with respect to the slope is excellent, even if our values are a bit too low by about 200 keV (see Fig. 6). The results from the most recent calculations from Ref. [41], depicted as the (green) dashed line, shows a similar behavior as our prediction, with a notch in the total γ-ray energy at the threshold for second-chance fission. In contrast, the data from Ref. [27], corresponding to the dotted line in Fig. 6, do not exhibit any kinks at all in the vicinity of the thresholds for second- and third-chance fission, which should appear, if the evaporation of neutrons prior to fission had been corrected for. In Ref. [29] it was shown that both components, i.e., pre-fission neutrons and neutrons emitted from fission fragments, add up to the total average prompt-fission neutron multiplicity, which is given in evaluated data libraries and which in fact is usually measured in dedicated experiments. Hence, pre-fission neutrons must be subtracted from these data when the de-excitation of fission fragments is considered.

Here we find it appropriate to motivate why only neutron evaporation was taken into account in our treatment of pre-fission neutrons. There is another process occurring above around 10-MeV incident neutron energy, namely so-called pre-equilibrium emission, in which the first neutron is emitted before complete equilibrium is established, with an average energy of $\approx E_n - B_f$ [49]. In that work prompt-fission neutron spectra are shown, calculated with on the basis of different theoretical models, for ${}^{232}\mathrm{Th}(n,f)$, ${}^{235}\mathrm{U}(n,f)$, and ${}^{239}\mathrm{Pu}(n,f)$, respectively. Among other energies, $E_n \approx 14$ MeV was chosen, an incident neutron energy highly relevant for this work. A close inspection of those spectra, e.g., for ${}^{235}\mathrm{U}(n,f)$ reveals that pre-equilibrium neutrons are emitted with a probability of approximately 0.6 %. For the other systems shown in Ref. [49] the situation is very similar, which is why we do not see any reason not to apply it to ${}^{238}\mathrm{U}(n,f)$ as well. In comparison, pre-fission evaporation neutrons amount about 20% of all prompt-fission neutrons at that particular incident neutron energy. Hence, for $E_n = 14$ MeV the increase of average energy of the first pre-fission neutron amounts to only about 200 keV, which causes a deviation of the pre-fission neutron multiplicity of at most 1% over the entire neutron energy region up to 20 MeV. Comparing this with other uncertainties, like the somewhat big ones from the fits to the experimental data in the systematics, we conclude that pre-equilibrium neutron emission is indeed negligible for the calculation of PFGS characteristics in the energy range considered in this work.

The best agreement was observed between our predictions and the results from the most recent calculation from Ref. [41], although no kink is observed there at the threshold for third-chance fission (see Fig. 6). The weak decrease in the calculated values above 18 MeV is from the onset of fourth-chance fission, which was not taken into account in our calculations. A conclusion that may be drawn from the discussion so far is that the choice of cross section data for the decomposition of the individual fission channels is affecting the energy dependence of $\overline{\nu}_{ff}$ and thus the shape of $E_{\gamma,\mathrm{tot}}(E_n)$. The appearance of kinks at the thresholds for higher chance fission channels was also observed for the systems $n + {}^{232}\mathrm{Th}$, $n + {}^{235}\mathrm{U}$, and $n + {}^{237}\mathrm{Np}$ [50], which may be seen as a confirmation of our predictions.

The experimental data that is currently available for the system $n + {}^{238}\mathrm{U}$ is not really helping to shed more light on the energy dependence of $E_{\gamma,\mathrm{tot}}$, because the values are still so few and also somewhat deviating. This is also the case in particular for the energy dependence of both average γ-ray energy and multiplicity, because here not even results from model calculations are available yet, except for one neutron energy. The most probable explanations for the observed differences are that experiments with fast neutrons are somewhat difficult to conduct because of the much lower neutron fluxes compared to thermal neutron fluxes from a research reactor and, most of all, that fission cross sections are more than two orders of magnitudes lower for fast neutrons. Both, for a similar amount of beam time, deteriorate statistics, which makes it more difficult to select prompt-fission γ rays from other events and to unfold the detector response. Because the fast-neutron induced reactions, for which experimental results exist, are the first of their kind, we believe that this will improve with time, i.e., with further experimental efforts.

As shown in the previous section, there are two approaches to describe the behavior of the average γ-ray energy ϵ_γ with incident neutron energy (see Fig. 8). Which approach is the more realistic one is hard to tell so far. However, the measurement of prompt-fission neutron spectra as a function of incident neutron energy would provide information about the energy release by these neutrons, which together with the kinetic energies of the fission fragments should help to answer that question.

Nevertheless, our predictions build on reasonable assumptions, which in principle may easily be transferred to any fissioning system. This way predictions can quickly be made, e.g., for estimating γ-ray count rates when proposing new experiments. So far they are still suffering from considerable uncertainties, basically from the fits of the systematics in Sec. II. The poor quality of the fits there, caused by the limited number of experiments that could have been taken into consideration, is most probably also responsible for the difference of about 200 keV in average total γ-ray energy. This is also reflected by the differing results published earlier [25,26] compared to this work, where already more experimental data were available. However, even more, reliable experimental data included in the systematics will certainly reduce the uncertainties of the fit parameters and, hence, of the predictions.

Anyway, we have shown that the systematics, which was originally found for thermal-neutron induced and spontaneous fission [1], may as well be applied to fission induced by fast neutrons as long as the corresponding prompt-fission neutron multiplicities are known and correctly used. For the system $n + {}^{238}\mathrm{U}$ new experimental results are under way. Recent measurements, performed at the LICORNE facility of IPN Orsay [46], were covering the energy region $E_n =$ 4–8 MeV. The analysis of the collected data is in progress. Another experimental campaign with LICORNE is scheduled for the end of 2016, dedicated to the system $n + {}^{239}\mathrm{Pu}$ in the incident neutron energy range $E_n = 0.5$–4 MeV. Calculations corresponding to those presented here have already been performed for this new system, and the results are waiting for experimental proof.

Also new experimental efforts on thermal-neutron induced and spontaneous fission, preferably on nuclides other than covered so far, are needed to provide a broader basis for revised systematics of PFGS properties and thus for predictions with higher precision. Last but not least it should be pointed out that it is definitely desirable to replace the purely empirical A and Z dependencies by physical ones, for which the support of theoreticians is crucial.

ACKNOWLEDGMENTS

One of the authors (R.B.) is indebted to the European Commission for providing a Ph.D. fellowship at EC-JRC IRMM, during which part of this work was carried out. A.O. acknowledges the support from the Extreme Light Infrastructure Nuclear Physics (ELI-NP) Phase II, a project co-financed by the Romanian Government and the European Union through the European Regional Development Fund—the Competitiveness Operational Programme (1/07.07.2016, COP, ID 1334), with which this work had been finalized.

[1] T. E. Valentine, Ann. Nucl. Energy **28**, 191 (2001).
[2] F. Pleasonton, Nucl. Phys. A **213**, 413 (1973).
[3] F. Pleasonton, R. L. Ferguson, and H. W. Schmitt, Phys. Rev. C **6**, 1023 (1972).
[4] V. V. Verbinski, H. Weber, and R. E. Sund, Phys. Rev. C **7**, 1173 (1973).
[5] R. W. Peelle and F. C. Maienschein, Phys. Rev. C **3**, 373 (1971).
[6] F. Pleasonton, R. L. Ferguson, and H. W. Schmitt, Oak Ridge National Laboratory, Report No. ORNL-4844, 109-112 (1972).
[7] H. R. Bowman and S. G. Thompson, in *Proceedings 2nd International Conference on Peaceful Uses of Atomic Energy, United Nations, Geneva*, Vol. 15 (International Atomic Energy Agency, Vienna, 1958), p. 212 .
[8] E. Nardi, A. Gavron, and Z. Fraenkel, Phys. Rev. C **8**, 2293 (1973).
[9] G. V. Val'skii, B. M. Aleksandrov, I. A. Baranov, A. S. Krivokhatskii, G. A. Petrov, and Yu S. Pleva, Sov. J. Nucl. Phys. **10**, 137 (1969).
[10] Nuclear Data High Priority Request List of the NEA (Req. ID: H.3, H.4), www.oecd-nea.org/dbdata/hprl/hprlview.pl?ID=421; www.oecd-nea.org/dbdata/hprl/hprlview.pl?ID=422.
[11] R. Billnert, F.-J. Hambsch, A. Oberstedt, and S. Oberstedt, Phys. Rev. C **87**, 024601 (2013).
[12] A. Oberstedt, R. Billnert, F.-J. Hambsch, and S. Oberstedt, Phys. Rev. C **92**, 014618 (2015).
[13] A. Oberstedt, T. Belgya, R. Billnert, R. Borcea, T. Bryś, W. Geerts, A. Göök, F.-J. Hambsch, Z. Kis, T. Martinez, S. Oberstedt, L. Szentmiklosi, K. Takàcs, and M. Vidali, Phys. Rev. C **87**, 051602(R) (2013).
[14] A. Gatera, F. J. Hambsch, A. Oberstedt, and S. Oberstedt, Proceedings of Theory-4 Scientific Workshop on Nuclear Fission Dynamics and the Emission of Prompt Neutrons and Gamma Rays, Varna, Bulgaria, June 20–22, 2017, EPJ Web of Conferences (in press).
[15] A. Gatera, T. Belgya, W. Geerts, A. Göök, F.-J. Hambsch, M. Lebois, B. Maroti, A. Moens, A. Oberstedt, S. Oberstedt, F. Postelt, L. Qi, L. Szentmiklosi, G. Sibbens, D. Vanleeuw, M. Vidali, and F. Zeiser, Phys. Rev. C **95**, 064609 (2017).
[16] S. Oberstedt, R. Billnert, T. Belgya, T. Bryś, W. Geerts, C. Guerrero, F.-J. Hambsch, Z. Kis, A. Moens, A. Oberstedt, G. Sibbens, L. Szentmiklosi, D. Vanleeuw, and M. Vidali, Phys. Rev. C **90**, 024618 (2014).
[17] S. Oberstedt, A. Oberstedt, A. Gatera, A. Göök, F.-J. Hambsch, A. Moens, G. Sibbens, D. Vanleeuw, and M. Vidali, Phys. Rev. C **93**, 054603 (2016).
[18] A. Chyzh, C. Y. Wu, E. Kwan, R. A. Henderson, J. M. Gostic, T. A. Bredeweg, R. C. Haight, A. C. Hayes-Sterbenz, M. Jandel, J. M. O'Donnell, and J. L. Ullmann, Phys. Rev. C **85**, 021601(R) (2012).
[19] A. Chyzh, C. Y. Wu, E. Kwan, R. A. Henderson, J. M. Gostic, T. A. Bredeweg, A. Couture, R. C. Haight, A. C. Hayes-Sterbenz, M. Jandel, H. Y. Lee, J. M. O'Donnell, and J. L. Ullmann, Phys. Rev. C **87**, 034620 (2013).
[20] A. Chyzh, C. Y. Wu, E. Kwan, R. A. Henderson, T. A. Bredeweg, R. C. Haight, A. C. Hayes-Sterbenz, H. Y. Lee, J. M. O'Donnell, and J. L. Ullmann, Phys. Rev. C **90**, 014602 (2014).
[21] J. L. Ullmann, E. M. Bond, T. A. Bredeweg, A. Couture, R. C. Haight, M. Jandel, T. Kawano, H. Y. Lee, J. M. O'Donnell, A. C. Hayes, I. Stetcu, T. N. Taddeucci, P. Talou, D. J. Vieira, J. B. Wilhelmy, J. A. Becker, A. Chyzh, J. Gostic, R. Henderson, E. Kwan, and C. Y. Wu, Phys. Rev. C **87**, 044607 (2013).
[22] www.oecd-nea.org/science/wpec/sg40-cielo/.
[23] H. Nifenecker, C. Signarbieux, M. Ribrag, J. Poitou, and J. Matuszek, Nucl. Phys. A **189**, 285 (1972).
[24] M. Heil, R. Reifarth, M. M. Fowler, R. C. Haight, F. Käppeler, R. S. Rundberg, E. H. Seabury, J. L. Ullmann, J. B. Wilhelmy, and K. Wisshak, Nucl. Instrum. Methods A **459**, 229 (2001).
[25] A. Oberstedt, R. Billnert, and S. Oberstedt, Proceedings of NEMEA-7 The 7th Workshop on Nuclear Measurements, Evaluations and Applications, November 5–8, 2013, Geel, Belgium, OECD Nuclear Science Report No. NEA/NSC/DOC 13, 199–209 (2014).
[26] A. Oberstedt, P. Halipré, F.-J. Hambsch, M. Lebois, S. Oberstedt, and J. N. Wilson, Phys. Proc. **64**, 91 (2015).
[27] D. G. Madland, Nucl. Phys. A **772**, 113 (2006).
[28] ENDF/B-VII.1 Evaluated Nuclear Data Files ZA=92238, NSUB=10(N), MT=456 (2011), www.nndc.bnl.gov/exfor/endf02.jsp.
[29] Chen Yong-Jing and Liu Ting-Jin, Chin. Phys. C **35**, 344 (2011).

[30] K. S. Krane, *Introductory Nuclear Physics* (John Wiley & Sons, New York, 1988).
[31] ENDF/B-VII.1 Evaluated Nuclear Data Files ZA=92237, NSUB=10(N), MT=456 (2011), www.nndc.bnl.gov/exfor/endf02.jsp.
[32] ENDF/B-VII.1 Evaluated Nuclear Data Files ZA=92236, NSUB=10(N), MT=456 (2011), www.nndc.bnl.gov/exfor/endf02.jsp.
[33] ENDF/B-VII.1 Evaluated Nuclear Data Files ZA=92238 and 92237, NSUB=10(N), MT=18 (2011), www.nndc.bnl.gov/exfor/endf02.jsp.
[34] ENDF/B-VII.1 Evaluated Nuclear Data Files ZA=92238, NSUB=10(N), MT=20 (2011), www.nndc.bnl.gov/exfor/endf02.jsp.
[35] JENDL-4.0 Evaluated Nuclear Data Files ZA=92238, NSUB=10(N), MT=20 (2011), www.nndc.bnl.gov/exfor/endf02.jsp.
[36] G. Vladuca, F.-J. Hambsch, A. Tudora, S. Oberstedt, A. Oberstedt, F. Tovesson, and D. Filipescu, Nucl. Phys. A **740**, 3 (2004).
[37] O. Litaize and O. Serot, Phys. Rev. C **82**, 054616 (2010).
[38] D. Regnier, O. Litaize, and O. Serot, Phys. Proc. **47**, 47 (2013).
[39] O. Litaize, O. Serot, D. Regnier, and C. Manailescu, Nucl. Data Sheets **118**, 216 (2014).
[40] O. Litaize, D. Regnier, and O. Serot, Phys. Proc. **59**, 89 (2014).
[41] A. Tudora (private communication).
[42] A. Tudora, Ann. Nucl. Energy **53**, 507 (2013).
[43] A. Tudora, F.-J. Hambsch, and S. Oberstedt, Nucl. Phys. A **890**, 77 (2012).
[44] J.-M. Laborie, G. Belier, and J. Taieb, Phys. Proc. **31**, 13 (2012).
[45] J.-M. Laborie, R. Billnert, G. Bélier, A. Oberstedt, S. Oberstedt, and J. Taieb (unpublished).
[46] M. Lebois, J. N. Wilson, P. Halipré, B. Leniau, I. Matea, A. Oberstedt, S. Oberstedt, and D. Verney, Nucl. Instrum. Methods A **735**, 145 (2014).
[47] M. Lebois, J. N. Wilson, P. Halipré, A. Oberstedt, S. Oberstedt, P. Marini, C. Schmitt, S. J. Rose, S. Siem, M. Fallot, A. Porta, and A.-A. Zakari, Phys. Rev. C **92**, 034618 (2015).
[48] M. Lebois (private communication).
[49] R. Capote *et al.*, Nucl. Data Sheets **131**, 1 (2016).
[50] J. Fréhaut, Proceedings of a Consultants Meeting on Physics of Neutron Emission in Fission, May 24–27, 1988, Mito City, Japan, IAEA INDC(NDS)-220, 99.